

# Alloy softening in Ni<sub>3</sub>Al polycrystals

X. R. QIAN, Y. T. CHOU

*Department of Materials Science and Engineering, and Materials Research Center, Lehigh University, Bethlehem, PA 18015, USA*

The alloying effect of boron on localized deformation in Ni<sub>3</sub>Al polycrystals containing 24–26 at% Al was studied using microhardness indentation. Alloy softening was observed both along the grain boundaries and in the grain interior. The softening effect decreased as the aluminium concentration increased. For alloys of near-stoichiometric composition, the maximum effect occurred at about 0.23 at% (500 wt p.p.m.) boron. A softening mechanism based on cross slip of screw dislocations was proposed.

## 1. Introduction

It has been recognized that the addition of solute atoms in the range of a few parts per million in a high purity bcc metal may decrease its flow stress, a phenomenon known as “alloy softening”. Both substitutional and interstitial atoms, including self-interstitials, have been found to cause the softening effect, which for bcc metals occurs in the temperature range below 0.15  $T_m$  (melting point temperature). This interesting phenomenon has been reviewed by Christian [1], Ulitschny *et al.* [2] and Pink and Arsenault [3]. The latter two have summarized most of the data available at the time. It appears that alloy softening is a general feature in bcc alloys at low temperatures, e.g. in Fe–Ni/Se [4], Mo–Re [5], Fe–C [6], Fe–N [7] and ordered TiNi [8]. More recently, alloy softening has also been observed in boron-doped Ni<sub>3</sub>Al, an ordered intermetallic alloy with L1<sub>2</sub> structure [9].

For Ni<sub>3</sub>Al alloy, boron was found to be effective in improving its ductility and fabricability [10, 11]. A considerable interest was stimulated in exploiting the possible mechanism for the boron effect. Recent investigations include boron segregation at grain boundaries [12] and at antiphase boundaries [13], and the effect of boron on slip propagation across the grain boundary [14]. It has been postulated [15] that boron exhibits a significant strengthening effect in Ni<sub>3</sub>Al due to the large lattice strain produced by the boron atoms. However, on the grain boundaries, addition of boron would cause a softening effect due to the emission of grain boundary dislocations [16]. According to Weihs *et al.* [17], the addition of boron would harden the coarse-grained alloys, but soften the fine-grained alloys (< 10  $\mu\text{m}$ ). This indicates that boron would soften the boundary but not the grain.

In recent studies on localized deformation using microhardness indentation [9, 18, 19], it was found that the addition of boron (500 wt p.p.m. or 0.23 at%) in a polycrystalline Ni<sub>3</sub>Al would soften both grain boundary and grain interior. (In our earlier work [18, 19], the boron concentration was rounded off at 0.2 at%). The purpose of the present investigation is

to extend the earlier work and to consider the effects of alloy stoichiometry and boron concentration on boron-induced softening.

## 2. Experimental procedure

The Ni<sub>3</sub>Al intermetallic alloys used in this study were supplied by the Oak Ridge National Laboratory. Their compositions are listed in Table I. The as-cast alloys (Nos. 1–6) were rod shaped with a diameter of  $\sim 10$  mm. A homogenization treatment was carried out in which the samples were vacuum encapsulated ( $\sim 10^{-2}$  torr) in fused silica tubes, heated at  $1200 \pm 10^\circ\text{C}$  for a period of 72 h and furnace cooled to room temperature. The homogenized alloys have an average grain size of about 0.9 mm as used in the previous study. Alloys Nos. 7–11 were heat treated at  $1050^\circ\text{C}$  for 2 h in vacuum ( $10^{-5}$  torr). The average grain size was about 0.3 mm.

Annealed samples were cut from each alloy (1–6) at three different angles with the longitudinal axis, i.e. at  $45^\circ$ ,  $90^\circ$  and  $180^\circ$ . To minimize the error due to surface preparation, a set of six samples from two alloy sets (three boron-free and three boron-doped) was mounted in a bakelite mould. For alloys 7–11, a set of four samples was mounted in a mould. The mounts were mechanically ground to 600 grit emery papers, then polished with 6  $\mu\text{m}$  diamond paste and 0.3  $\mu\text{m}$  alumina powder. In order to obtain reliable microhardness data, the mounts were further polished with 0.05  $\mu\text{m}$  silicon dioxide. Finally, they were chemically etched in a solution containing equal parts of HNO<sub>3</sub>, H<sub>2</sub>SO<sub>4</sub>, and H<sub>3</sub>PO<sub>4</sub> by volume for 45 s. Vickers hardness (DPH) was measured on a Tukon microhardness tester equipped with a microprocessor. The dependence of microhardness on indentation load was determined and two levels of loading were used. For grain interior, the load was 500 g and each data point obtained for an individual grain represented the average of five indentation readings. More indentations in a grain would result in interference from deformation in

adjacent indentation sites. The spacing of two adjacent indentations was chosen to be about six units of edge length of the indentation (Fig. 1a). The experimental errors involved in the measurements were

TABLE I Alloy compositions

Alloy No.	Composition (at %)		
	Al	B <sup>a</sup>	Ni
1	24	0	Bal.
2	25	0	Bal.
3	26	0	Bal.
4	24	0.23	Bal.
5	25	0.23	Bal.
6	26	0.23	Bal.
7	25.2	0	Bal.
8	25.2	0.09	Bal.
9	25.2	0.23	Bal.
10	25.2	0.47	Bal.
11	25.2	0.93	Bal.

<sup>a</sup> Values are converted from the wt % added in the alloy.

within  $\pm 3\%$ . For hardness measurements on grain boundaries, a load of 5 g was used, giving an indentation diagonal of 5–7  $\mu\text{m}$ . In this case, ten measurements were taken for each data point with an error of  $\pm 7\%$  (Fig. 1b.). A relatively short loading time (30 s) was chosen for both situations to minimize the errors due to the vibration of the hardness tester.

To compare the hardness of a grain boundary with that of the neighbouring interior, a 5 g load was used for both regions. As expected, the phenomenon of grain-boundary hardening exists for all the samples tested. Fig. 2 shows a typical hardness–distance profile near a grain boundary in a stoichiometric  $\text{Ni}_3\text{Al}$  alloy.

### 3. Results and discussion

#### 3.1. Experimental results on boron-induced softening

Figs 3–8 illustrate the frequency distributions of 30 averaged Vickers hardness numbers (DPH) in grain

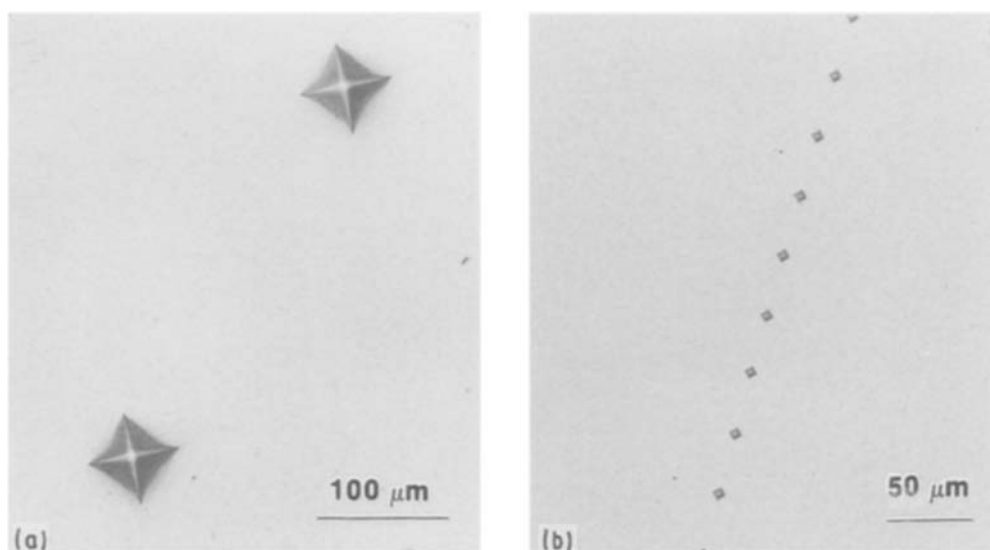


Figure 1 Vickers hardness indentations on stoichiometric  $\text{Ni}_3\text{Al}$  alloy with 0.23 at % boron. (a) In grain interior (500 g load); (b) on grain boundary (5 g load).

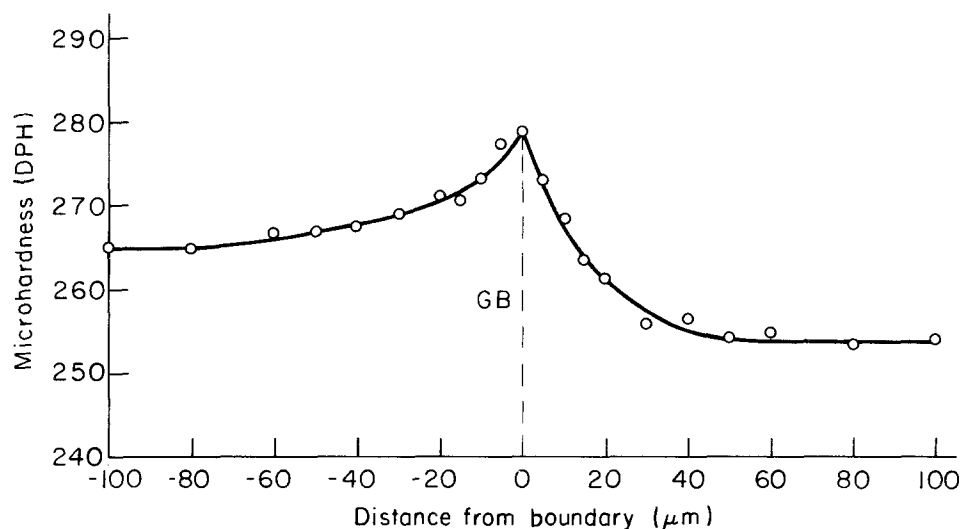


Figure 2 Hardness–distance profile near a grain boundary in a stoichiometric  $\text{Ni}_3\text{Al}$  alloy (5 g load).

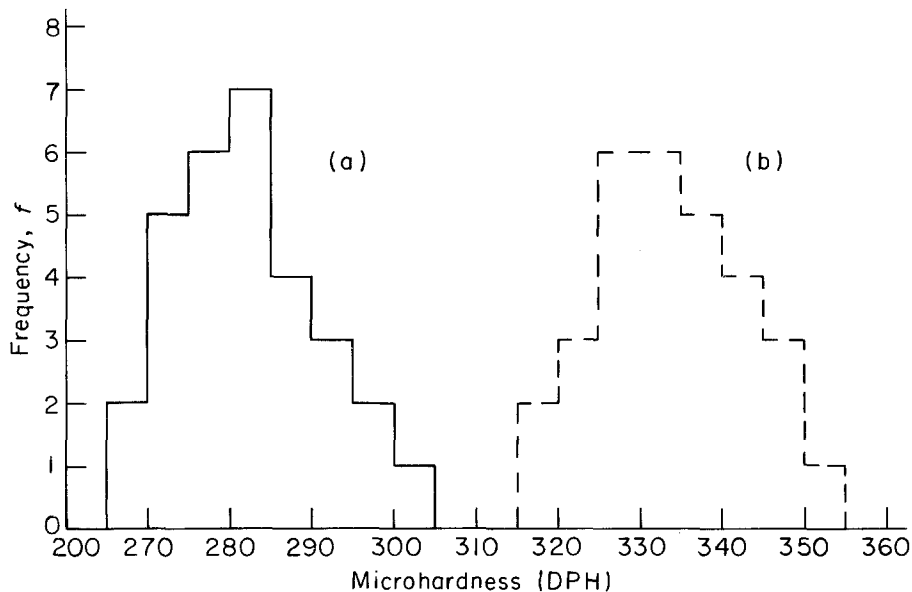


Figure 3 Frequency distributions of 30 averaged Vickers hardness numbers (DPH) on grain boundaries of a hypostoichiometric  $\text{Ni}_3\text{Al}$  alloy at a 5 g load. (a) Alloy doped with 0.23 at % boron (mean = 282.2); (b) boron-free alloy (mean = 333.8).

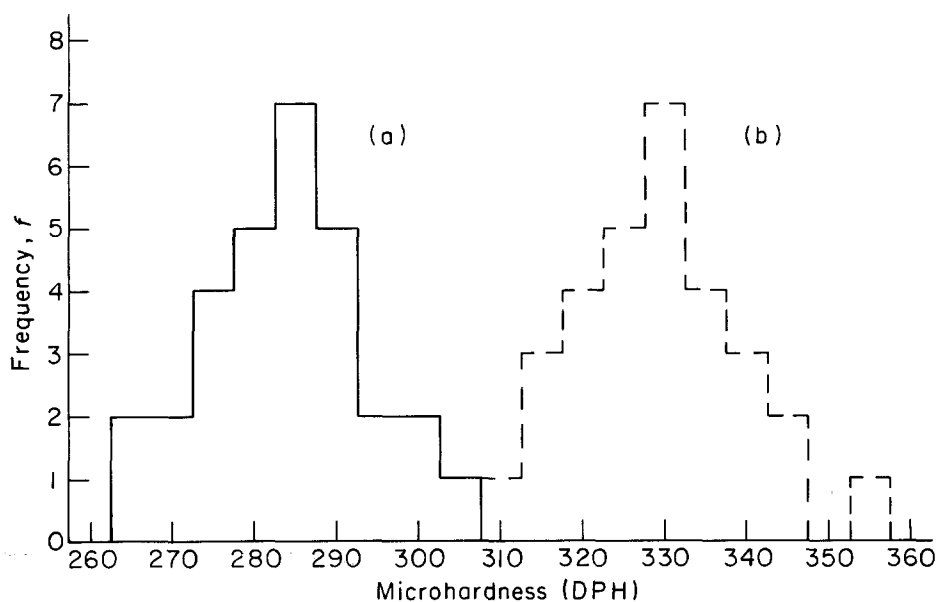


Figure 4 Frequency distributions of 30 averaged Vickers hardness numbers (DPH) in grain boundaries of a stoichiometric  $\text{Ni}_3\text{Al}$  alloy at a 5 g load. (a) Alloy doped with 0.23 at % boron (mean = 283.7); (b) boron-free alloy (mean = 329.2).

interiors (a total of 150 indentations) and on grain boundaries (a total of 300 indentations) for each of the stoichiometric and off-stoichiometric  $\text{Ni}_3\text{Al}$  alloys with and without boron. The 95% confidence intervals [19] for the population means ( $\mu$ ), standard deviations ( $\sigma$ ), and the differences between the means of boron-free and boron-doped alloys ( $\mu_F - \mu_D$ ) are shown in Tables II–IV respectively. The statistical data for alloys 1–6 show that the average microhardness of the boron-doped alloy is, in general, lower than that of the boron-free alloy, with the exception that for the hyperstoichiometric alloy (26 at % Al) the trend is reversed.

### 3.2. Grain-boundary softening and its stoichiometry dependence

The statistical means of microhardness on grain

boundaries and in grain interiors with and without boron are plotted in Figs 9 and 10 as a function of aluminium concentration. It is seen that with the addition of 0.23 at % (500 wt p.p.m.) of boron to  $\text{Ni}_3\text{Al}$ , the grain-boundary hardness was consistently decreased. This leads to the hypothesis that boron softens the grain boundaries in  $\text{Ni}_3\text{Al}$ . The experimental results support the argument by Schulson and co-workers [16, 20, 21] that the addition of boron reduces the effectiveness of grain boundary strengthening and increases the ease with which grain boundaries accommodate slip. A second point from the results is that the effect of boron on grain boundary hardness is dependent on alloy stoichiometry, i.e. the extent of grain boundary softening would decrease as the aluminium content varies from hypo- to hyperstoichiometric. This can be partially understood based

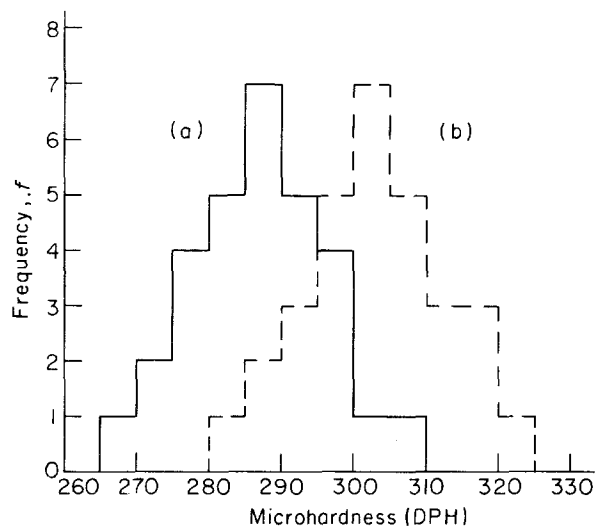


Figure 5 Frequency distributions of 30 averaged Vickers hardness numbers (DPH) on grain boundaries of a hyperstoichiometric  $\text{Ni}_3\text{Al}$  alloy at a 5 g load. (a) Alloy doped with 0.23 at % boron (mean = 287.0); (b) boron-free alloy (mean = 303.0).

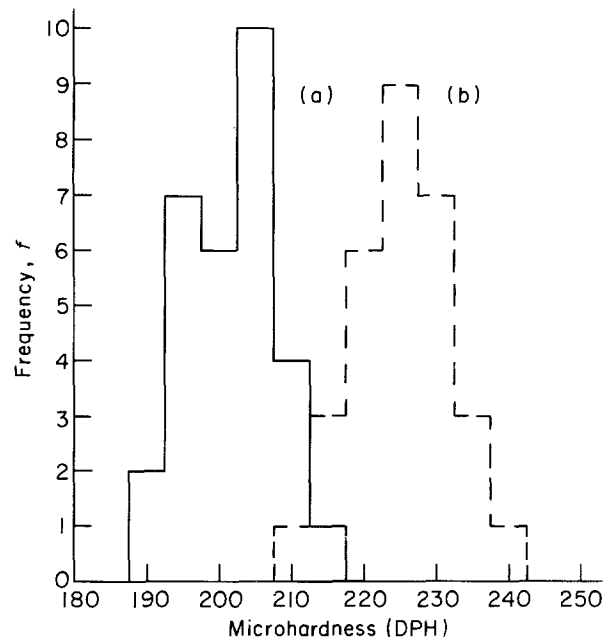


Figure 7 Frequency distributions of 30 averaged Vickers hardness numbers (DPH) on grain-interiors of a stoichiometric  $\text{Ni}_3\text{Al}$  alloy at a 500 g load. (a) Alloy doped with 0.23 at % boron (mean = 201.7); (b) boron-free alloy (mean = 225.2).

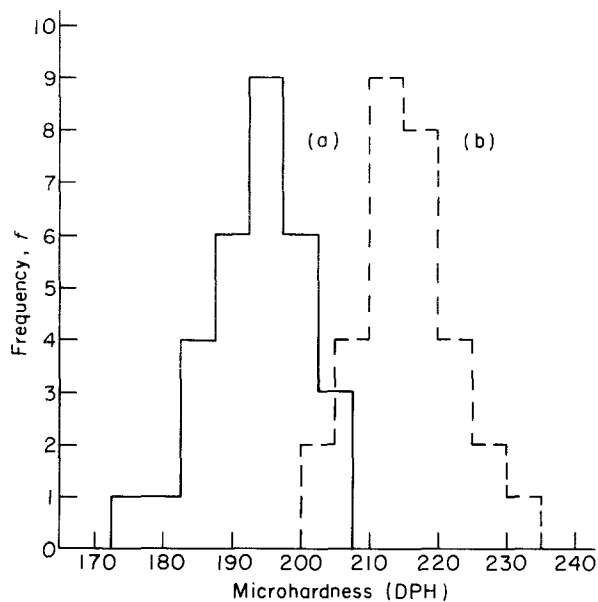


Figure 6 Frequency distributions of 30 averaged Vickers hardness numbers (DPH) in grain interiors of a hypostoichiometric  $\text{Ni}_3\text{Al}$  alloy at a 500 g load. (a) Alloy doped with 0.23 at % boron (mean = 193.5); (b) boron-free alloy (mean = 215.5).

on the effect of stoichiometry in boron segregation behaviour. The level of boron segregation at the grain boundaries decreases with increasing aluminium concentration in  $\text{Ni}_3\text{Al}$  [12, 22, 23]. That is, the boron becomes less effective in softening  $\text{Ni}_3\text{Al}$  if its content is less than a critical amount ( $\sim 10$  at % B) present at the grain boundaries.

The experimental data also show that in boron-free  $\text{Ni}_3\text{Al}$  alloys, the grain-boundary hardness decreases with increasing aluminium concentration, since aluminium is softer than nickel. In addition, Takasugi *et al.* [24] has concluded that grain boundary hardening with respect to the neighbouring grain interior is dependent on alloy stoichiometry. They postulated that when the excess Ni atoms substituted for Al atoms in the grain boundary region of a hypostoichio-

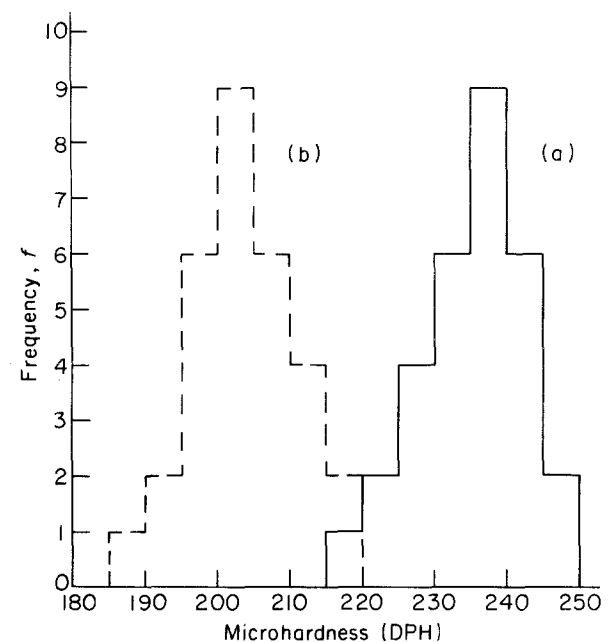


Figure 8 Frequency distributions of 30 averaged Vickers hardness numbers (DPH) in grain interiors of a hyperstoichiometric  $\text{Ni}_3\text{Al}$  alloy at a 500 g load. (a) Alloy doped with 0.23 at % boron (mean = 235.2); (b) boron-free alloy (mean = 203.7).

metric alloy, the Ni-Ni bonds produced would create more homogeneous charge distribution through the boundary plane, resulting in a higher grain boundary strength. This argument is consistent with our results.

### 3.3. Grain softening and the proposed mechanism of cross slip

Figs 6–8 demonstrate that small additions of boron can decrease microhardness in grain interiors as well, but only when the intermetallic is stoichiometric or

TABLE II 95% confidence intervals for statistical mean,  $\mu$ 

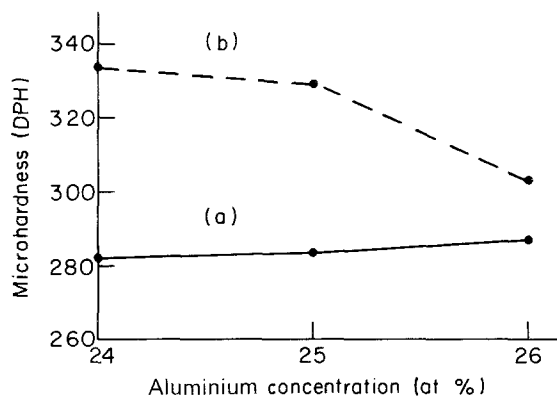
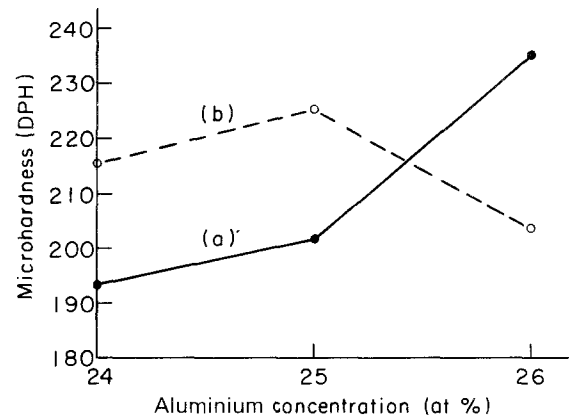
Micro-alloying	Composition (at %)					
	24Al GB <sup>a</sup>	GI <sup>b</sup>	25Al GB	GI	26Al GB	GI
Boron-free	(330.4, 337.2)	(212.8, 218.2)	(325.4, 333.0)	(222.6, 227.8)	(299.3, 306.7)	(200.0, 207.4)
0.23 at % boron	(278.8, 285.6)	(190.8, 196.2)	(280.0, 287.4)	(199.3, 204.1)	(283.6, 290.4)	(232.4, 238.0)

<sup>a</sup> GB, grain boundary.<sup>b</sup> GI, grain interior.TABLE III 95% confidence intervals for standard deviation,  $\sigma$ 

Micro-alloying	Composition (at %)					
	24Al GB <sup>a</sup>	GI <sup>b</sup>	25Al GB	GI	26Al GB	GI
Boron-free	(7.3, 12.6)	(5.6, 9.6)	(8.1, 14.1)	(5.5, 9.3)	(7.7, 13.4)	(5.8, 9.8)
0.23 at % boron	(7.1, 12.3)	(5.8, 9.8)	(7.9, 13.6)	(5.0, 8.5)	(7.3, 12.6)	(5.9, 10.0)

<sup>a</sup> GB, grain boundary.<sup>b</sup> GI, grain interior.TABLE IV 95% confidence intervals for the difference between the means of boron-free and boron-doped alloys ( $\mu_F - \mu_D$ )

	Composition (at %)					
	24Al GB <sup>a</sup>	GI <sup>b</sup>	25Al GB	GI	26Al GB	GI
( $\mu_F - \mu_D$ )	(49.3, 53.9)	(18.3, 25.7)	(20.1, 26.9)	(40.3, 50.7)	(11.1, 20.9)	(-27.7, -35.3)

<sup>a</sup> GB, grain boundary.<sup>b</sup> GI, grain interior.Figure 9 Effect of aluminium concentration on hardness along grain boundaries in  $Ni_3Al$ . (a) Alloy doped with 0.23 at % boron; (b) boron-free alloy.Figure 10 Effect of aluminium concentration on hardness in the grain interior in  $Ni_3Al$ . (a) Alloy doped with 0.23 at % boron; (b) boron-free alloy.

aluminium-lean. For hyperstoichiometric  $Ni_3Al$  alloy, only the strengthening effect was observed. It is commonly believed that in the  $Ni_3Al$  lattice, boron atoms reside interstitially and generate a lattice strain which imparts a marked increase in lattice resistance to slip. The present results show partially the opposite effect.

There are a number of mechanisms proposed for the alloy softening [25]. The two most popular are: (i) the reduction of the Peierls stress by solutes; and (ii) the enhancement of the rate of double-kink formation of screw dislocations as a result of the elastic interaction

with solute atoms [26]. These mechanisms are "intrinsic softening" mechanisms and imply that the dislocation mobility is determined by the Peierls lattice potential. Hence they are not applicable to fcc systems in which the dislocation-lattice interaction is expected to be small. For the present case, a different mechanism should be considered.

As mentioned in the review articles [27, 28], the dislocation structure in a deformed  $Ni_3Al$  alloy primarily consists of long, straight screw dislocations. The flow stress of  $Ni_3Al$  has a very unusual temperature

dependence, i.e. it increases with increasing temperature. This behaviour is the result of thermally-activated cross slip of  $a/2\langle 110 \rangle$  screw dislocations from the (111) planes, where they are mobile, to (010) planes, where they are immobile. At room temperature, the motion of the  $a/2 [\bar{1}01]$  superpartial dislocation on the (111) plane would result in the production of an APB (anti-phase boundary) on the same plane. This configuration (Fig. 11) is strongly pinned and the flow stress is increased (work hardening). Copley and Kear [29] and Pauder *et al.* [30] have shown that under the geometric considerations, cross slip from (111) to (1 $\bar{1}$ 1) planes without changing dislocation mobility is possible only for samples oriented near [001] at temperatures near the peak in the CRSS (critical resolved shear stress) against temperature plot. Cross slip can be neglected for the samples oriented at other orientations. On the other hand, although it is well known that most alloying additions to Ni<sub>3</sub>Al cause strengthening, it is possible that other alloying additions may result in weakening. Pope and Ezz [28] pointed out that the causes of these strengthening or weakening effects appear to be related to the anisotropy of the APB energy, which is the main driving force for cross slip from (111) to (010) planes. Suzuki *et al.* [31] have argued that the decrease in the positive temperature dependence of the flow stress is caused by a decrease in the APB energy on (111) planes as a result of the Fe addition. Wee and co-workers [32] suggested that alloying elements which tend to make a given L1<sub>2</sub> alloy unstable with respect to DO<sub>19</sub> or DO<sub>22</sub> (or other similar structures) will also decrease the APB energy on the (010) planes, which leads to an increase in the rate of cross slip from (111) to (010). In our case, where a certain content of boron is added to Ni<sub>3</sub>Al alloy, it can reasonably be

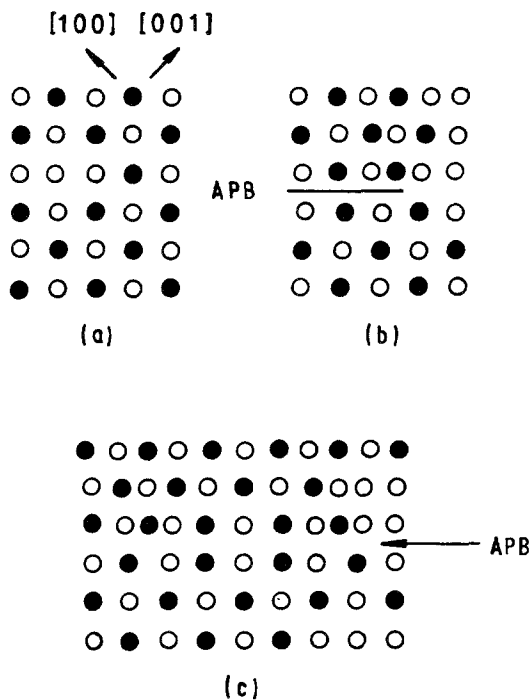


Figure 11 The anti-phase boundaries (APB) in L1<sub>2</sub> structure; (a) A (010) plane of a L1<sub>2</sub> structure; (b) as in (a) but with  $a/2 [101]$  dislocation on the (111) plane, producing an APB; (c) two  $a/2 [101]$  dislocations, as in (b), connected by an APB [28].

suggested that the energy of APB on the (111) plane is decreased. In the following analysis, an attempt will be made to show that the boron addition leads to alloy softening.

According to Gilman [33], the stress dependence of the dislocation velocity is given by

$$V = V^* \exp\left(-\frac{Db}{\Sigma f_i}\right), \quad \Sigma f_i \geq 0 \quad (1)$$

where  $V^*$  is the shear-wave velocity,  $D$  is a measure of the friction forces that act on the dislocation (called the characteristic drag-stress coefficient),  $b$  is the Burgers vector,  $f_i$  is the  $i$ th force acting on the dislocation, and  $\Sigma$  stands for summation. Consider a pair of superlattice partial dislocations associated with an APB on the (111) plane. The velocity of each superpartial is

$$V = V^* \exp\left(-\frac{Db}{\tau b - \gamma + \mu b^2/2\pi\Delta x}\right) \quad (2)$$

where  $\tau$  is the resolved shear stress,  $\gamma$  is the antiphase boundary energy,  $\mu b^2/2\pi\Delta x$  is repulsive force between two partials, and  $\Delta x$  is their equilibrium width. From Equation 2, a reduction of the APB energy on (111) planes would increase the velocity of the super partials. This means that the mobility of the superlattice screw dislocations would be increased and the rate of work-hardening decreased. Moreover, the frequency for cross slip from the (111) to the (010) plane would be decreased due to the decrease in the APB energy on the (111) plane, and weakening results. In L1<sub>2</sub> structure, there is a necessary condition for the cross slip from the (111) to the (010) plane [34], given by

$$\left(\frac{3A}{A+2}\right) \frac{\gamma_1}{\gamma_0} > 3^{1/2} \quad (3)$$

where  $A = 2c_{44}/(c_{11} - c_{12})$ ,  $c_{11}$ ,  $c_{12}$  and  $c_{44}$  are elastic constants, and  $\gamma_1$  and  $\gamma_0$  are the APB energies on {111} and {100} planes, respectively. Therefore the likelihood for a superpartial dislocation to cross slip from the (111) to the (010) plane will be decreased as  $\gamma_1$  is reduced.

On the other hand, the interaction between an interstitial dipole and superpartial screw dislocation will promote the cross slip from the (111) to the (1 $\bar{1}$ 1) plane and thus relax the flow stress. This mechanism has been used to explain the alloy softening in the Fe-N system near 175 K [35, 36]. Here only an illustrated description is presented. Fig. 12 shows the ( $\bar{1}01$ ) plane containing three {111} slip traces and three possible interstitial sites. The circles represent the equipotentials for the interaction when the Burgers vector is normal to the paper and the interstitial is at the type 3 site. The two other types of interstitial positions produce similar equipotential systems and the whole displays trigonal symmetry about the [ $\bar{1}01$ ] direction. While the dislocation is moving along [ $\bar{1}2\bar{1}$ ] on the (111) plane, the total energy increases and a retardation is experienced. Suppose that the dislocation now cross slips onto (1 $\bar{1}$ 1) along [ $12\bar{1}$ ]. Since this direction is down the gradient of the potential field, the interstitial assists glide on the new slip plane and, hence, promotes cross

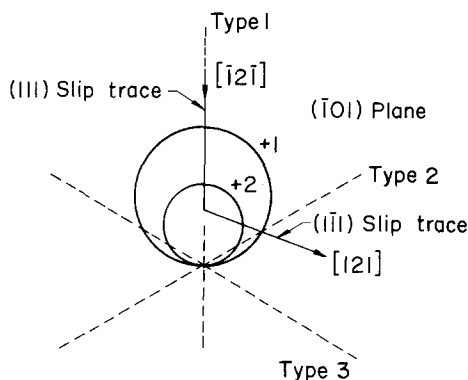
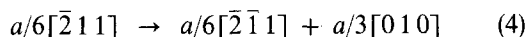


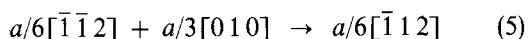
Figure 12 Schematic representation of cross slip from (111) to (1 $\bar{1}\bar{1}$ ) plane in Ni<sub>3</sub>Al.

slip. The forces depend not only on the type of the site, but also upon whether the interstitial is above or below the slip plane. Although the calculation indicates that only type 2 and 3 interstitial dipoles can produce an effect to promote cross slip of screw dislocations, there always exist circumstances when the properly oriented interstitial dipoles exert forces on the dislocations in a {111} cross-slip direction.

Assuming that the velocities of superpartial dislocations are represented by Equation 2, it is likely that if the leading dislocation should cross slip from the (111) into the (1 $\bar{1}\bar{1}$ ) plane, the trailing dislocation will almost certainly follow the same path into (1 $\bar{1}\bar{1}$ ). Cross slip may occur when a leading partial dislocation, with Burgers vector  $a/6 [2\bar{1}1]$ , dissociates into two partials, one of which,  $a/6 [\bar{2}\bar{1}1]$ , glides on the cross slip plane and the other,  $a/3 [010]$ , is sessile at the intersection of the two planes involved. The reaction is



Subsequently, the second of the partials originally on the primary slip plane is attracted to the sessile, and combines with it to give the second  $a/6[\bar{1}\bar{1}2]$  partial on the cross slip plane, i.e.



An approximate configuration just after Reaction 4 is shown in Fig. 13.

The relaxation of stress can occur by the cross slip mechanism. Once the double cross slip occurs, the Frank-Read source can begin to operate as described by Low and Guard [37], thus increasing the mobile dislocation density. Cross slip occurs where the dislocations are observed to multiply.

### 3.4. Competition between two deformation processes

Nakada and Keh [7] in their study of the Fe-N system remarked that alloy softening and alloy strengthening are two concurrent but competitive processes in the course of deformation. Under certain circumstances, alloy strengthening is the dominant mechanism, while in other situations alloy softening plays a superior role. The balance of the two processes

depends on the interplay of the process parameters, i.e. temperature, alloy concentration, crystallographic orientation, grain size, strain rate, etc. In the present case, for hypostoichiometric Ni<sub>3</sub>Al alloys, the softening effect of boron predominates over the strengthening effect. However, it has been suggested [38] that the defect trapping associated with 25 and 26 at % Al causes boron to cluster in the matrix, resulting in an increase in hardness with increasing aluminium concentration. In hyperstoichiometric alloys, the strengthening effect by clustering surpasses the boron softening, leading to apparent hardening (Fig. 8). Lopez and Hancock [39] showed that the excess Al or Ni in the Ni<sub>3</sub>Al structure resulted in a higher flow stress and that an excess of Al would have a much more marked effect than an excess of Ni. Rawlings and Stanton-Bevan [40] concluded that the extent of solid-solution strengthening resulting from the alloy addition depends on the atomic-misfit parameter, the stoichiometry of the alloy, and the substitutional nature of the element added. Elements with large misfits that substitute for Al in Al-rich alloys produce the most strengthening effect. Noguchi *et al.* [41] have studied the effects of deviation from stoichiometry on the flow stress of polycrystalline Ni<sub>3</sub>Al and Ni<sub>3</sub>Ga. They found that an excess of Al produces a greater increase in strength than does an excess of Ni. All these aforementioned experiments and arguments are consistent with our results.

### 3.5. Effect of boron concentration on alloy softening

The effect of boron concentration on hardness in Ni-25.2 at % Al alloys (samples 7-11) was also examined. As shown in Fig. 14, as the concentration of boron increases from zero to 2000 wtp.p.m., the microhardness first decreases and then increases through a minimum at 500 p.p.m. boron. This can be qualitatively explained based on the ease of cross slip [36]. At a very low concentration of interstitials, the dislocation can sweep forward on the primary slip plane since the interaction between a dislocation and a single interstitial is weak and is not able to promote

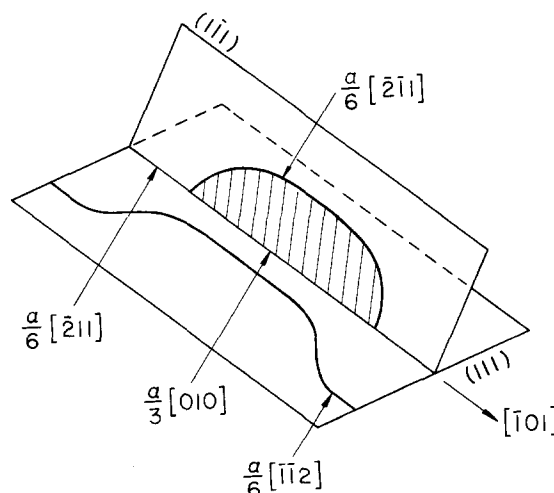


Figure 13 Cross-slip of an extended dislocation in Ni<sub>3</sub>Al.

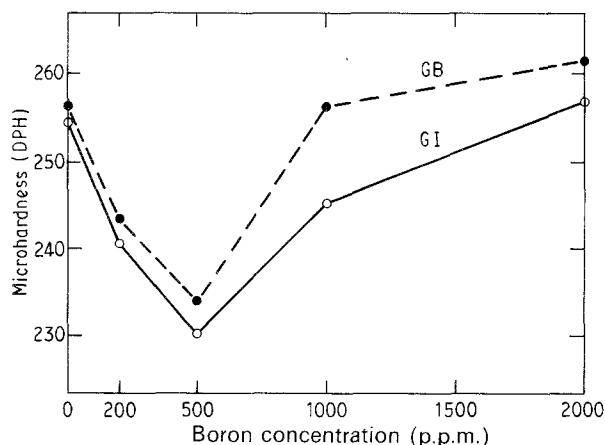


Figure 14 Dependence of boron concentration (wt p.p.m.) on hardness of Ni-25.2 at % Al alloy. (GB), grain boundary; (GI), grain interior.

cross slip. When more interstitials are present and are situated so close together that the distance of forward sweeping is less than one Burgers vector, the dislocation would remain straight and cross slip would then take place by the cooperative action of several interstitials. However when the interstitial concentration is too high, the likelihood that a large number of interstitials are all acting on the dislocation in the same way is negligible. Thus cross slip ought not be significant at this high level of concentration. This would explain why the cross-slip frequency goes through a maximum and the hardness through a minimum as the concentration of boron increases. Chaki [42] has recently proposed a bond-distortion model for boron softening in the  $\text{Ni}_3\text{Al}$  lattice. According to his analysis, an amount of 3900 at p.p.m. ( $\sim 830$  wt p.p.m.) of boron would be needed to fully effect the softening process. This level of boron content, however, was not studied in the present investigation.

It should be pointed out that the above experimental results do not coincide completely with the compiled data for room temperature tensile yield strengths of  $\text{Ni}_3\text{Al}$  alloys with and without boron [14, 16]. On macrostraining (tensile loading) of  $\text{Ni}_3\text{Al}$  alloy softening occurs only in the smaller grain size range ( $< 10 \mu\text{m}$ ) and strengthening in a large grain-size range. The salient point of the present investigation is to show that on microstraining (hardness) alloy softening seems to be a general phenomenon and is independent of grain size. It appears that more studies, especially TEM analyses, are needed to clarify the role of boron in the localized deformation of  $\text{Ni}_3\text{Al}$  alloys.

#### 4. Conclusions

1. Alloy softening was observed in  $\text{Ni}_3\text{Al}$  polycrystals due to the addition of boron. The degree of softening decreases with increasing aluminium concentration.

2. Alloy softening in the grain interior is not present in the hyperstoichiometric alloy of 26 at % Al, probably due to the competition between the boron-induced cluster strengthening and the boron-induced cross slip softening. In the hyperstoichiometric alloy,

boron clusters were found in the grain and the balance is thus tipped toward hardening.

3. In stoichiometric alloys with different boron concentrations, the maximum softening effect appears near 0.23 at % (500 wt.p.p.m.) boron.

#### Acknowledgements

The authors wish to thank Dr C. T. Liu and Dr D. M. Kroeger of the Oak Ridge National Laboratory for helpful discussions. The work was sponsored by the Division of Materials Sciences, Office of Basic Energy Sciences, US Department of Energy under Grant DE02-86ER45256.

#### References

1. J. W. CHRISTIAN, Proceedings of the 2nd International Conference on Strength of Metals and Alloys, Vol. 1 (American Society of Metals, Metals Park, OH, 1970) p. 29.
2. M. G. ULITCHNY, A. A. SAGUES and R. GIBALA, in "Defects in Refractory Metals", edited by R. de Baptist, J. Nihoul and L. Stals (SCK. CENMol, Belgium, 1972) p. 245.
3. E. PINK and R. J. ARSENAULT, *Progr. Mater. Sci.* **24** (1979) 1.
4. T. TANAKA and S. WATANABE, *Acta Metall.* **19** (1971) 991.
5. J. R. STEPHENS and W. R. WITZKE, *J. Less-common Metals* **29** (1972) 371.
6. Z. S. BASINSKI and J. W. CHRISTIAN, *Aust. J. Phys.* **13** (1960) 299.
7. Y. NAKADA and A. S. KEH, *Acta Metall.* **16** (1968) 903.
8. M. GARFINKLE, *Metall. Trans.* **5** (1974) 2383.
9. X. R. QIAN and Y. T. CHOU, in Proceedings of the Materials Research Society's Symposium on Interfacial Structure, Properties, and Design, edited by M. H. Yoo, C. L. Briant and W. A. T. Clark (Materials Research Society Press, Pittsburgh, 1988) p. 311.
10. K. AOKI and O. IZUMI, *Nippon Kinzoku Gakkaishi* **43** (1979) 1190.
11. C. T. LIU and C. C. KOCH, "Technical Aspects of Critical Materials used by the Steel Industry", Vol. 11B, NBSIR 83-2679-9 (National Bureau of Standards, Gaithersburg, MD, 1983).
12. C. T. LIU, C. L. WHITE and J. A. HORTON, *Acta Metall.* **33** (1985) 213.
13. J. A. HORTON and M. K. MILLER, *ibid.* **35** (1986) 133.
14. P. S. KHADKIKAR, K. VEDULA and B. S. SHABEL, *Metall. Trans.* **18A** (1987) 425.
15. S. C. HUANG, A. I. TAUB and K. M. CHANG, *Acta Metall.* **32** (1984) 1703.
16. E. M. SCHULSON, T. P. WEIHS, I. BAKER, H. J. FROST and J. A. HORTON, *ibid.* **34** (1986) 1395.
17. T. P. WEIHS, V. ZINOVIEV, D. V. VIENS and E. M. SCHULSON, *ibid.* **35** (1987) 1109.
18. X. R. QIAN and Y. T. CHOU, *Mater. Lett.* **6** (1988) 157; *Scripta Met.* **22** (1988) 725.
19. *Idem.*, in Proceedings of the Materials Research Society's Symposium on High Temperature Ordered Intermetallic Alloys, edited by C. C. Koch, C. T. Liu, N. S. Stoloff and A. I. Taub (Materials Research Society Press, Pittsburgh, PA 1989) p. 529.  
(Note: The captions for this paper, Figs 1 and 2 should be interchanged).
20. I. BAKER, E. M. SCHULSON and J. A. HORTON, *Acta Metall.* **35** (1987) 1533.
21. E. M. SCHULSON, I. BAKER and H. J. FROST, in Proceedings of the Materials Research Society's Symposium on High Temperature Ordered Intermetallic Alloys II, edited by N. S. Stoloff, C. C. Koch, C. T. Liu and O. Izumi (Materials Research Society Press, Pittsburgh, PA 1987) p. 195.
22. A. I. TAUB, S. C. HUANG and K. M. CHANG, in Proceedings of the 39th Meeting of the Mechanical Failure Prevention



- Group, edited by J. G. Early, T. R. Shivers and J. H. Smith (Cambridge University Press, New York, 1985) p. 57.
23. C. T. LIU, C. L. WHITE, C. C. KOCH and E. H. LEE, in Proceedings of the Electrochemical Society on High Temperature Materials, edited by Munir Cubicciotti (Electrochemical Society, 1983) p. 32.
  24. T. TAKASUGI, N. MASAHASHI and O. IZUMI, *Acta Metall.* **35** (1987) 381.
  25. H. MATSUI and H. KIMURA, *Mater. Sci. Engng* **40** (1979) 207.
  26. A. SATO and M. MESHII, *Acta Metall.* **21** (1973) 753.
  27. N. S. STOLOFF and R. G. DAVIES, *Prog. Mater. Sci.* **13** (1966) 3.
  28. D. P. POPE and S. S. EZZ, *Int. Metall. Rev.* **29** (1984) 136.
  29. S. M. COPLEY and B. H. KEAR, *Trans. AIME* **239** (1967) 977.
  30. V. PAIDAR, D. P. POPE and V. VITEK, *Acta Metall.* **32** (1984) 435.
  31. T. SUZUKI, Y. OYA and D. M. WEE, *ibid.* **28** (1980) 301.
  32. D. M. WEE, O. NOGUCHI, Y. OYA and T. SUZUKI, *Trans. Jpn Inst. Met.* **21** (1980) 237.
  33. J. J. GILMAN, *J. Appl. Phys.* **36** (1965) 3195.
  34. M. H. YOO, in Proceedings of the Materials Research Society's Symposium on High Temperature Ordered Intermetallic Alloys II, edited by N. S. Stoloff, C. C. Koch, C. T. Liu and O. Izumi (Materials Research Society Press, Pittsburgh, PA 1987) p. 207.
  35. B. W. CHRIST, *Acta Metall.* **17** (1969) 1317.
  36. C. L. FORMBY, *Phil. Mag.* **14** (1966) 745.
  37. J. R. LOW, Jr. and R. W. GUARD, *Acta Metall.* **7** (1959) 171.
  38. A. DASGUPTA, L. C. SMEDSKJAER, D. G. LEGNIKI and R. W. SIEGEL, *Mater. Lett.* **3** (1985) 457.
  39. J. A. LOPEZ and G. F. HANCOCK, *Phys. Status Solidi (a)* **2** (1970) 469.
  40. R. D. RAWLINGS and A. STATON-BEVAN, *J. Mater. Sci.* **10** (1975) 505.
  41. O. NOGUCHI, Y. OYZ and T. SUZUKI, *Metall. Trans.* **12A** (1981) 1647.
  42. T. K. CHAKI, *Phil. Mag. Lett.* **61** (1990) 5.

*Received 25 October 1990  
and accepted 28 February 1991*